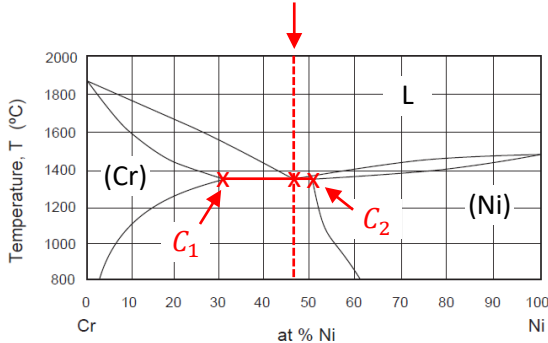


**Q1. Phase diagrams**

(a) Cr-Ni alloy of eutectic composition:  
 relative atomic weights  $a_{Cr} = 52.0$ ,  $a_{Ni} = 58.7$

(i) Eutectic point:  $C_0 = 47$  at% Ni,  $T = 1355$  °C



(ii) Just below the eutectic:

(Cr) phase:  $C_1 = 31$  at% Ni (Cr rich solid)

(Ni) phase:  $C_2 = 51$  at% Ni (Ni rich solid)

Compositions, in wt% Ni:  $\text{kg of Ni} = \text{kmol of Ni} \times \text{kg/kmol}$

$$C_0 = \frac{47(58.7)}{47(58.7) + 53(52.0)} = 50 \text{ wt\% Ni}$$

$$C_1 = \frac{31(58.7)}{31(58.7) + 69(52.0)} = 34 \text{ wt\% Ni}$$

$$C_2 = \frac{51(58.7)}{51(58.7) + 49(52.0)} = 54 \text{ wt\% Ni}$$

Proportions by weight: use the lever rule, ensuring the compositions are in wt%

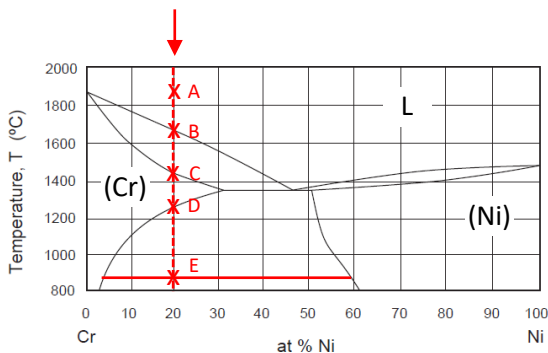
$$F_{(Cr)} = \frac{C_2 - C_0}{C_2 - C_1} = \frac{54 - 50}{54 - 34} = 0.2$$

$$F_{(Ni)} = \frac{C_0 - C_1}{C_2 - C_1} = \frac{50 - 34}{54 - 34} = 0.8$$

Comments:

- Take care not to confuse the *composition* of a phase (i.e. the fraction of Ni in that phase) and the *proportion* of a phase (i.e. the fraction of that phase in the two phase mixture).
- The lever rule applies equally well to concentrations expressed in wt% and at%. But the former gives the proportions by weight, as required (the latter gives the proportions by number of atoms).
- Applying the lever rule *by measurement* only works if the axis is linear in wt% (if you want the proportions by weight) or linear in at% (if you want the proportions by number of atoms). Because we want proportions by weight, and the axis is linear in at%, measurement doesn't work here.

(b) Alloy Cr-20at% Ni cooled slowly from 1800 °C:



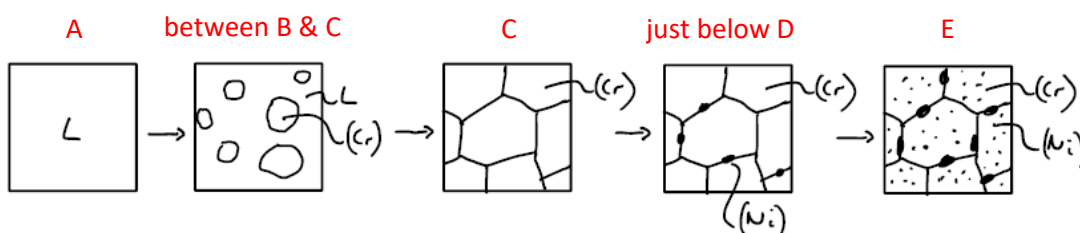
A - 100% liquid (L)

B - Solid (Cr) starts to nucleate and grow within the liquid. On further cooling, the proportion of solid increases (following the lever rule).

C - 100% solid (Cr).

D - Saturation limit for (Cr); (Ni) precipitation begins.

E - Increasing fraction of (Ni) precipitates in (Cr), as given by the lever rule. Compositions of these phases also change on cooling, as given by the ends of the tie line.

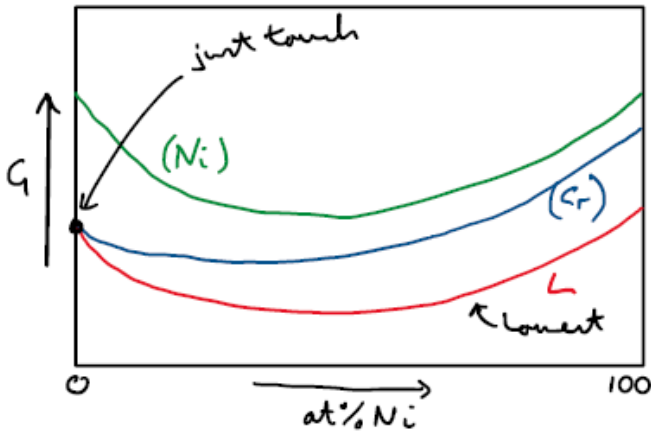


Comments:

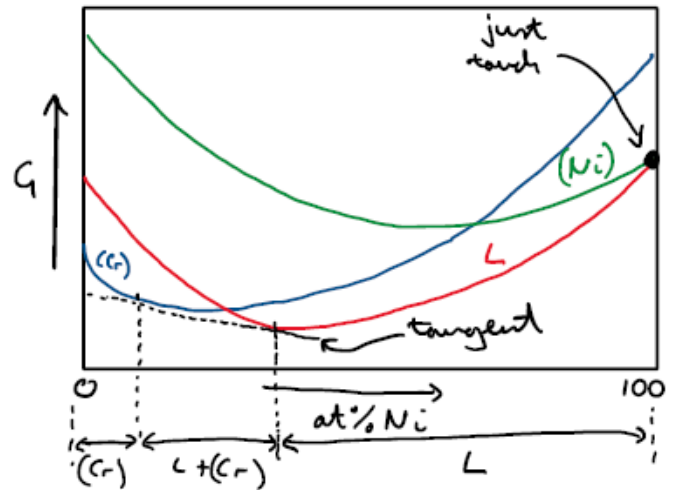
- Don't forget to discuss the full temperature range requested. It was common to omit the changes occurring on cooling below point D.
- Because this passes through the 100% (Cr) region, the transformation at D is *precipitation* of (Ni) out of (Cr), and not the *eutectic* transformation discussed in part (a).

(c) Variation in Gibbs free energy with composition, at selected temperatures:

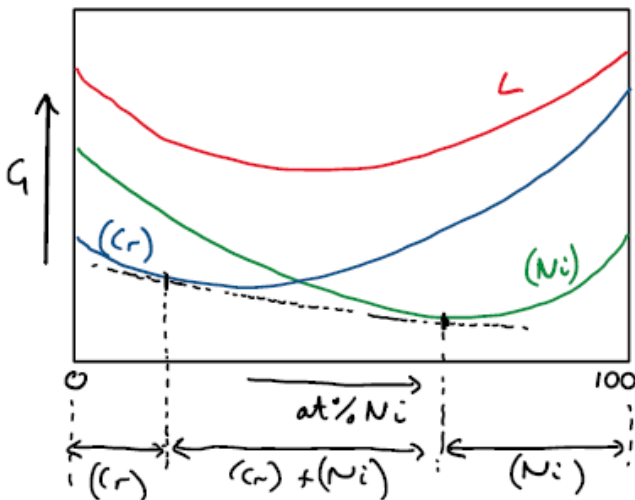
(i) Melting temperature of pure Cr



(ii) Melting temperature of pure Ni



(iii) 1000 °C



Comments:

- The key thing being assessed here is that the relationship between the curves is approximately right, and that the shape of the curves (u-shaped) is approximately right. Precise details of where the curves meet the axes, or locations of minima etc, were not expected.
- Showing clearly that liquid and solid curves just touch, as marked above, was necessary to get full marks for (i) and (ii).
- Note that the edges of the two phase regions in (ii) and (iii) are defined by where the common tangent touches the two curves, and not by the minima of the curves.
- A thorough answer should also note which phase or mixture of phases is stable (i.e. has the lowest G) over each composition range, at each temperature.

## Q2. Solidification and casting

(a) Solidification of pure aluminium:

(i) At a temperature  $T$ , the free energy difference between solid and liquid:  $\Delta G = \Delta H - T\Delta S$

$$\text{At } T = T_m: \quad \Delta G = \Delta H - T_m\Delta S = 0 \quad \therefore \Delta S = \frac{\Delta H}{T_m}$$

$$\text{Near to } T_m: \quad \Delta S \approx \frac{\Delta H}{T_m} \quad \therefore \Delta G = \Delta H - T \left( \frac{\Delta H}{T_m} \right) = \Delta H \left( \frac{T_m - T}{T_m} \right)$$

(ii) Homogeneous nucleation:

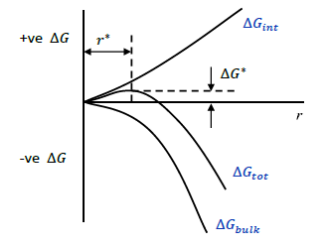
$$\text{Change (negative) in } G \text{ on forming a volume of solid: } \Delta G_v = \Delta H_v \left( \frac{T_m - T}{T_m} \right) = -|\Delta H_v| \left( \frac{T_m - T}{T_m} \right)$$

$$\text{Change (positive) in } G \text{ per unit area of solid-liquid interface: } \Delta G_{int} = \gamma$$

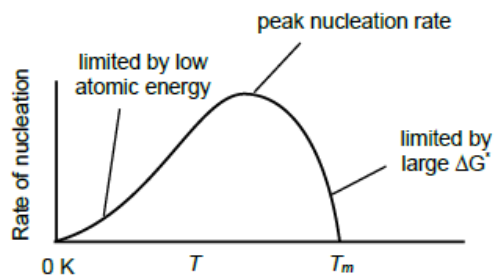
$$\text{Total change in free energy: } \Delta G_{tot} = \gamma (4\pi r^2) - |\Delta H_v| \left( \frac{T_m - T}{T_m} \right) \left( \frac{4}{3}\pi r^3 \right)$$

The critical radius occurs when  $\Delta G_{tot}$  is a maximum. At this size (even though  $\Delta G_{tot}$  is positive), increasing  $r$  further will tend to reduce  $\Delta G_{tot}$ , driving growth:

$$\frac{\partial \Delta G_{tot}}{\partial r} = \gamma (8\pi r) - |\Delta H_v| \left( \frac{T_m - T}{T_m} \right) (4\pi r^2) = 0 \quad \therefore r^* = \frac{2\gamma T_m}{|\Delta H_v| (T_m - T)}$$

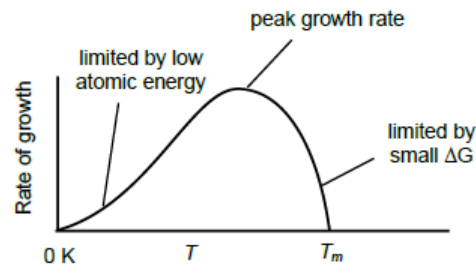


(iii) Rate of **nucleation**:



large  $\Delta G^*$ , few critical nuclei  $\rightarrow$  rate is low.

Rate of **growth** of stable nuclei:



small  $\Delta G \Rightarrow$  small bias in free energy  $\rightarrow$  rate is low.

- Rate of nucleation and rate of growth both follow (different) C-curves
- **Overall rate** of solidification depends on both of these, and so also follows a C-curve

Comments:

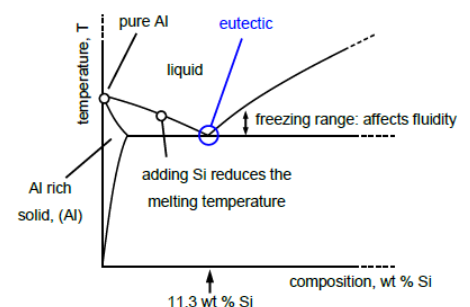
- Take care with the sign of  $\Delta G_v$  and  $\Delta H_v$  in (ii). Both will be negative, for the liquid to solid transformation below  $T_m$ . It therefore sometimes helps to write  $\Delta H_v = -|\Delta H_v|$  to clarify this.
- A good answer to (iii) discussed the trade-off between thermodynamic driving force ( $\Delta G$ , which is small at low undercooling) and diffusion rates (slow at large undercooling). Better answers drilled down further into the effect undercooling has on each of the two stages of transformation: nucleation and growth.

(b) Al-Si casting:

(i) Effect of adding Si (near eutectic is the target for casting):

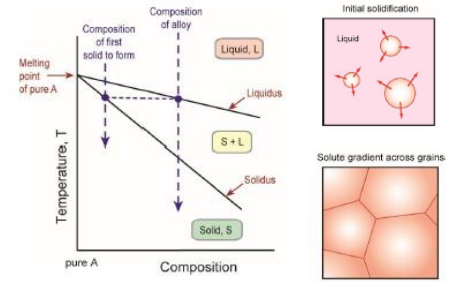
Processability: reduced  $T_m$ , reduced freezing range (a large freezing range can lead to fluidity problems, as the solid crystals increase the viscosity).

Properties: the two phase microstructure of Al rich solid and Si is harder but more brittle than pure Al.



(ii) Segregation:

- The development of a concentration gradient on solidification.
- This happens because the first solid to form has a lower concentration than the last, according to the tie line on the phase diagram (see right). If following equilibrium, the concentration of the solid will gradually change, by diffusion. However, in practise, diffusion is too slow for this to occur, so a concentration gradient remains trapped in the solid. Impurities can also remain trapped in the last liquid to solidify.



- Scales of segregation:

**Grain level** – from the centre of the grain, i.e. the initial nucleus (low concentration, the first solid to form) to the grain boundary (high concentration, the last solid to form).

**Casting level** – from the mould wall (low concentration, the first solid to form), to the centre (high concentration, the last solid to form).

(iii) Reducing segregation:

- add inoculants as sites for heterogeneous nucleation: leads to a reduced grain size, and hence reduced concentration gradients.
- homogenisation: heat up the casting to redistribute atoms by diffusion.

Comments:

- A common mistake in (i) was to confuse alloying for **casting** (this question) with alloying for **heat treatment** (covered in Q4). Si is not added for reasons of hardenability or age hardening - these are concepts linked to heat treatment.
- A sketch (like the figure above), with some bullet point comments, is an efficient and effective way to answer part (ii). There were a number of unnecessarily lengthy essays that made it difficult to see the key points clearly.

### Q3. Deformation processing

(a) Deformation processing vs casting:

Advantages of deformation processing:

- better surface finish & dimensional accuracy
- choice of alloy: wrought alloys tend to have good strength, toughness and ductility, whereas cast alloys can be hard but brittle
- work hardening can increase the strength (at the cost of some ductility)
- lower processing temperatures (not melting the material).

Alloy suitability:

- ductile enough to avoid cracking
- yield strength that is not too high, so tool forces are acceptable.

(b) Frictionless compression:

(i) Constant volume deformation: plastic deformation occurs by the glide of dislocations along slip planes, driven by shear stresses, which requires no volume change.

(ii) Conservation of volume:  $h_0 w_0 = hw$

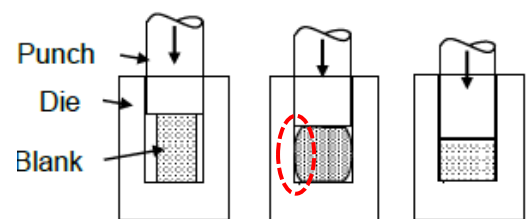
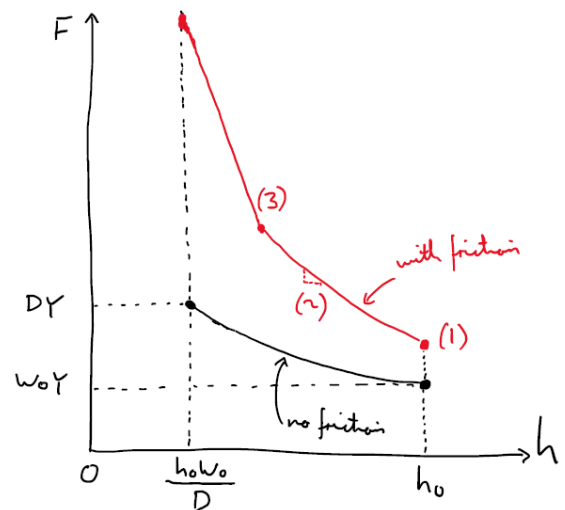
Force (per unit depth):  $F = wY = \left(\frac{h_0 w_0}{h}\right) Y$

(c) Adding Coulomb friction:

(i) (1) The initial force required to yield is higher (due to the presence of a horizontal stress  $\sigma_x$  now required to balance the frictional shear stresses - see below).

(2) The curve will rise more steeply with reducing  $h$ , as the effect of friction is more pronounced for small  $h/w$  (the peak of the 'friction hill' increases).

(3) In practice, friction would resist sliding at the interface, so the block would not retain a rectangular shape during compression (called 'barrelling'). The material would make contact with the sides of the die sooner than in the frictionless case. At this point, the force would start to rise more steeply due to the additional frictional resistance.

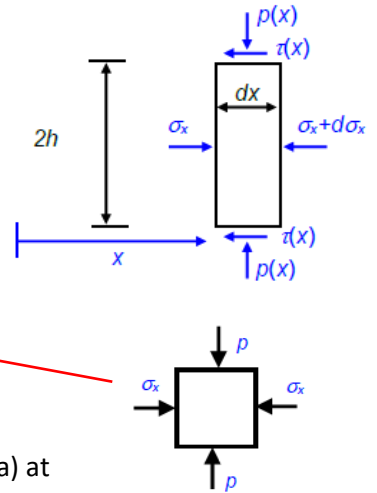


Comments:

- Part (b) is an unfamiliar analysis, but is based on the familiar concept that force = true stress x current area. Take care not to overcomplicate things by attempting the equilibrium analysis method from part (c)(ii), below. This is only necessary in the presence of friction, as this causes the stress state to vary through the block, and so requires analysis of a small element and integration. Without friction, the stress state is uniform everywhere, so a force balance for the whole block works OK.
- The comment (3) on 'barrelling' in (c)(i) might be deduced, but isn't really discussed in the course, so was not expected in the solution.

(ii) Equilibrium method:

- Resolve forces horizontally for a strip of material. **Assume** horizontal stress  $\sigma_{xx}$  is uniform through the height  $h$ . Gives a differential equation relating  $(\sigma_{xx}, \tau)$ .
- Friction law:  $\tau = \mu p$ . Substituting in now gives a differential equation relating  $(\sigma_x, p)$ .
- Yield criterion: **assume**  $\tau$  is relatively small, and so  $(\sigma_x, p)$  are approximately the principal stresses. Substituting the yield criterion in gives a differential equation now just in terms of  $p$ .
- Integrate to find  $p(x)$ . Boundary conditions:  $\sigma_x = 0$  ( $\therefore p = Y$ , using Tresca) at the free edge,  $x = w/2$ .



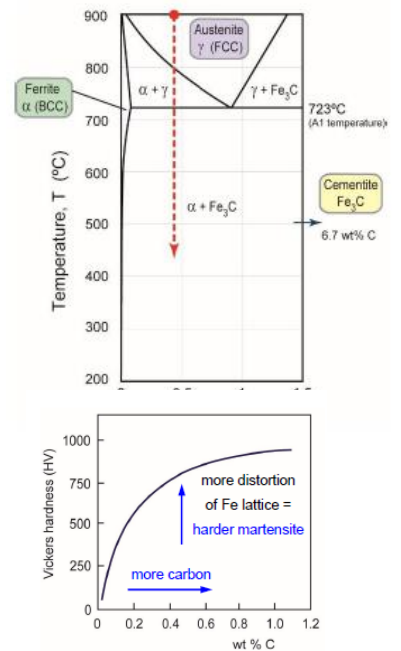
Comments:

- Many answers omitted comments on the modelling assumptions.
- Note that the solution obtained using this equilibrium analysis (which was not required here) supports points (1) and (2) in (c)(i).



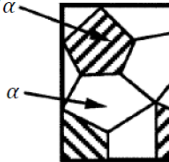
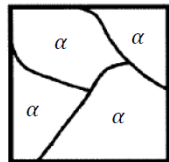
#### Q4. Heat treatment of steels

(a) Factors that affect the hardness of plain carbon steels:

- Hardness (which is related to the yield stress) is determined primarily by the microstructure of the steel, which in turn depends on the composition (i.e. the carbon content) and the thermal history.
- **Thermal history:** The microstructure forms as the steel cools from the austenite region of the phase diagram. The phase formation depends primarily on the solid state diffusion (thermally activated) of carbon atoms, and so depends on temperature and time. Decreasing the transformation temperature of steels generally results in a finer distribution of the cementite phase, from coarse pearlite (higher temperatures), to fine pearlite, to bainite (lower temperatures). Bainite has a higher hardness than coarse pearlite. For transformations at even lower temperatures diffusion is limited, and so the martensite phase transformation will occur instead. Here, all the carbon is trapped in solid solution. This phase has the highest hardness.
- **Carbon content:** For hypo-eutectoid steels, the carbon content influences the **proportions** of ferrite and pearlite in the steel. Pearlite is a harder microstructure than ferrite, due to the presence of the cementite phase ( $\text{Fe}_3\text{C}$ ), which has a high hardness. As the carbon concentration of the alloy approaches the eutectoid composition, the proportion of pearlite increases, and the hardness increases. For hyper-eutectoid steels, with carbon concentrations greater than the eutectoid composition, there will be a mixture of pearlite and cementite. The hardness will therefore be higher again. Increasing the carbon content will also increase the **hardenability** of the steel, i.e. it will reduce the cooling rates at which harder phases such as bainite and martensite form. The hardness of the martensite will also increase with carbon content, due to the increased solid solution hardening.

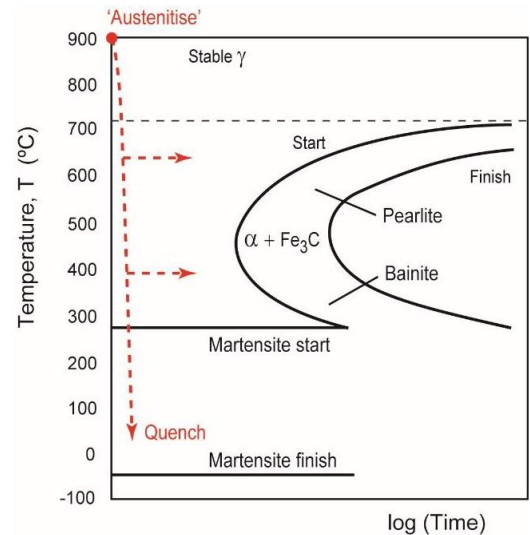


(b) Microstructures in order of decreasing hardness:

highest hardness			lowest hardness
 <p>(ii)</p>	 <p>(iii)</p>	 <p>(i)</p>	 <p>(iv)</p>
100% martensite ( $\alpha'$ )	100% pearlite, which is alternating ferrite ( $\alpha$ ) and cementite ( $\text{Fe}_3\text{C}$ )	~50% ferrite ( $\alpha$ ), 50% pearlite ( $\alpha + \text{Fe}_3\text{C}$ )	100% ferrite ( $\alpha$ )
High hardness due to high level of solid solution hardening - all of the C is trapped in solid solution.	Hardness due to the high proportion of the hard cementite phase.	The ferrite phase has a lower hardness than the pearlite, so (i) has a lower hardness than (iii).	Low hardness due to the low carbon content in ferrite.
0.8 wt% C, as this has the same composition as (iii)	0.8 wt% C, the eutectoid composition	~0.4 wt% C, applying the lever rule to the phase diagram just above the eutectoid temperature.	< 0.01 wt% C, from the 100% $\alpha$ region of the phase diagram

(c) TTT diagrams:

- TTT diagrams relate the time and temperature to the fraction of a phase transformed. They apply to isothermal (i.e. constant temperature) transformations only.
- For diffusive phase transformations, the TTT diagram takes the form of c-curves of % transformed. At higher temperatures, transformation rates are low (and therefore transformation times are large), due to the low undercooling and hence low thermodynamic driving force. But diffusion is more rapid, so microstructures tend to be coarse, equilibrium microstructures - for example **microstructure (iii)**.
- At lower temperatures, the rate of transformation is also low, due to the slower diffusion. Microstructures tend to be finer - e.g. bainite.
- Peak transformation rates (and minimum transformation times - the 'nose' of the c-curves) occurs between these extremes.
- TTT diagrams for steels also show fraction transformed contours for martensite at lower temperatures - **microstructure (ii)**.
- The martensite transformation occurs without diffusion, so the fraction transformed is independent of time - they are horizontal lines on the TTT diagram. However, the fraction transformed does depend on temperature, as increasing the undercooling increases the thermodynamic driving force for transformation, and increases the proportion of martensite that can form.



TTT diagram: eutectoid steel

(d) Steel for railway tracks:

- Fine eutectoid pearlite, microstructure (iii) when formed just above the nose of the c-curves, or tempered martensite, which is microstructure (ii) after holding at an elevated temperature for a period of time to enable diffusion of carbon, both give a good trade-off between yield strength (~500 MPa) and toughness (~50 MPa√m).
- Tempered martensite consists of extremely small and finely dispersed cementite particles embedded within a continuous ferrite matrix.
- Fine eutectoid pearlite is harder than lower carbon steels due mainly to the increased cementite content. Also the cementite-ferrite boundaries restrict dislocation motion, and hence plastic deformation of the softer ferrite phase.

Comments:

- Generally well attempted. The errors were primary in describing the time-temperature histories to achieve various microstructures, and in identifying some of the microstructures that had been sketched.
- A common problem was imprecise answers on the factors that govern the hardness of steels.



## Q5. Diffusion

(a) Parameters that affect the rate of diffusion of copper within aluminium:

- The net flux of atoms is proportional to the diffusion coefficient  $D = D_0 \exp(-Q/RT)$ . This increases with the temperature  $T$ . The diffusion constant  $D_0$  and the activation energy  $Q$  will depend on the atoms involved, in this case Cu and Al, and the mechanism of diffusion, in this case substitutional (rather than interstitial).
- Atoms move by diffusion via a statistical process, i.e. the probability to hop into an available site. A 'driving force' is necessary to tip the balance, to lead to a net flux of atoms in one direction. This could be a concentration gradient, i.e. Fick's first law:

$$J = -D \frac{dC}{dx}$$

or a stress field, or a concentration of vacancies, etc.

(b) Applications of diffusion:

(i) *Heat treatable Al alloys*: Diffusion is responsible for ageing in heat-treatable Al alloys. In this case, precipitates grow with time via diffusion, which alters their ability to resist the motion of dislocations. A peak in hardness is observed when these precipitates reach a critical size. The ageing temperature affects the rate of nucleation and growth of these precipitates, and hence the time required to reach this peak hardness.

(ii) *Doping semiconductors*: Doping allows the conductivity of semiconductors to be changed, by diffusing dopant atoms into silicon. For example, replacing a Si atom with a phosphorous atom leaves the covalent bond with one extra electron (n-type), and replacing a Si atom with a boron atom leave the covalent bond short of one electron, leaving a hole (p-type). Dopant atoms diffuse into the Si in two stages: pre-deposition (maintaining a high concentration at the surface) and drive-in (removing the dopant source, to achieve a more uniform distribution).

(c) Doping with boron: (i) Governing differential equation: 1D diffusion is governed by Fick's second law,

$$\frac{\partial C}{\partial t} = D \frac{\partial^2 C}{\partial x^2}$$

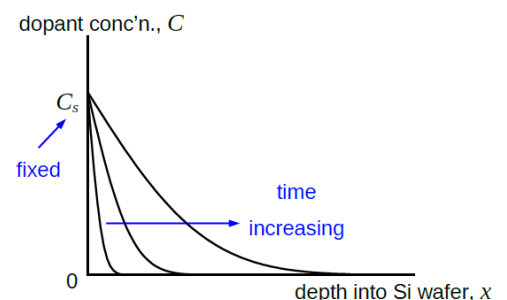
Its physical basis is conservation of mass. It can be derived by considering a small element of material, and balancing the net flux of atoms in with the increase in the total concentration in the element. The atomic flux is in turn modelled using Fick's first law (above).

(ii) The initial conditions are:  $C = 0$  at  $t = 0$ ,  $x \geq 0$

The boundary conditions are:  $C = C_s$  at  $x = 0$ ,  $t \geq 0$

This is the decaying step solution, modelled using the error function (Materials Data Book):

$$\frac{C}{C_s} = 1 - \operatorname{erf}\left(\frac{x}{2\sqrt{Dt}}\right)$$



(iii) The concentration at a given  $x$  and  $t$  depends on the non-dimensional group:  $x/2\sqrt{Dt}$

If the penetration depth  $x$  for a given concentration  $C$  is fixed, then  $\sqrt{Dt}$  is also fixed, and so:

$$\frac{t_1}{t_2} = \frac{D_2}{D_1} = \exp\left(-\frac{Q}{RT_2}\right) / \exp\left(-\frac{Q}{RT_1}\right) = 47$$

where  $T_2 = 1200 + 273 = 1473 \text{ K}$  and  $T_1 = 1000 + 273 = 1273 \text{ K}$ .

Comments:

- The main errors were in explaining the dependence of diffusion rate on temperature, and in writing the error function solution for 1D diffusion based on the given initial conditions.
- Also, a large number of students made numerical errors in using the activation energy to calculate the time ratios in (c)(iii) as they used inconsistent units for  $Q$  and  $RT$ .

## Q6. Creep

(a) Creep mechanisms:

- Both power-law and diffusional creep are described by:  $\dot{\epsilon} = A \sigma^n \exp\left(-\frac{Q}{RT}\right)$
- **Power law creep** occurs at  $T > 0.4T_m$  and relatively high stresses, with  $\dot{\epsilon}$  very stress dependent ( $n = 3 - 10$ ). The mechanism of power law creep is diffusion enabling dislocations to climb onto a different slip plane and continue to glide, overcoming obstacles.
- **Diffusional creep** also occurs at  $T > 0.4T_m$  but at lower stress levels, and is less stress sensitive ( $n = 1$ ). The mechanism is the diffusion of atoms along grain boundaries or through the bulk of the grains.

(b) Achieving creep resistance in alloys:

- **Melting temperature:** the rate of diffusion at a given temperature depends on  $T/T_m$ , so alloys with a high  $T_m$  (e.g. nickel alloys) will undergo lower creep rates, for both power law and diffusional creep.
- **Grain boundaries:** these offer relatively easy diffusion paths for atoms, and so reducing or eliminating grain boundaries (e.g. by casting single crystals) reduces the diffusional creep rate.
- **Obstacles to dislocations:** power law creep occurs by dislocations climbing to overcome obstacles. Increasing the density of obstacles, (e.g. by alloying to produce strong and stable precipitates, as in nickel superalloys) will reduce the creep rate for this mechanism.

(c) (i) At  $t = 0$ : the true stress  $\sigma = W/A_0$

Substituting into the given relationship, the initial true strain rate:

$$\dot{\epsilon}_{ss} = \dot{\epsilon}_0 \left( \frac{W}{A_0 \sigma_0} \right)^n$$

(ii) For  $t > 0$ : the true stress  $\sigma = W/A$  where  $A(t)$  is the current cross-sectional area. Note that  $W$  is constant (as specified in the question). The true strain rate at any instant is therefore

$$\dot{\epsilon} = \dot{\epsilon}_0 \left( \frac{W}{A \sigma_0} \right)^n$$

Conservation of volume gives:  $AL = A_0L_0$

$$\therefore \dot{\epsilon} = \dot{\epsilon}_0 \left( \frac{L W}{A_0 L_0 \sigma_0} \right)^n = \dot{\epsilon}_{ss} \left( \frac{L}{L_0} \right)^n$$

Note that  $\dot{\epsilon}_{ss}$  is a constant. The true strain rate is given by the rate of change of the current length / current length:

$$\dot{\epsilon} = \frac{1}{L} \frac{dL}{dt}, \quad \therefore \frac{1}{L} \frac{dL}{dt} = \dot{\epsilon}_{ss} \left( \frac{L}{L_0} \right)^n$$

Rearrange and integrate, noting that at  $t = 0$  the length  $L = L_0$ , and at rupture ( $t = t_f$ ) the area  $A \rightarrow 0$  and so the length  $L \rightarrow \infty$  from conservation of volume (in the absence of necking):

$$\int_{L_0}^{\infty} \frac{dL}{L^{n+1}} = \frac{\dot{\epsilon}_{ss}}{L_0^n} \int_0^{t_f} dt \quad \therefore t_f = \frac{1}{\dot{\epsilon}_{ss} n}$$

(iii) The above analysis neglects the onset of

- alternative failure modes (e.g. void growth and coalescence),
  - necking instabilities causing strain localisation,
- prior to the whole bar thinning to a zero cross-sectional area. For this reason, it is an upper bound.

Comments:

- Most answered the qualitative parts of the question well, but had difficulties with the calculation of the time to failure. A particular difficulty was setting up the integration in (c)(ii). Also, the fact that the true stress changes as the cross-sectional area decreases was missed.